



Ancient clays support contemporary biogeochemical activity in the Critical Zone

Vanessa M. Alfonso¹, Peter M. Groffman^{1,2}, Zhongqi Cheng¹, David E. Seidemann¹

5

¹Department of Earth and Environmental Sciences, Brooklyn College of the City University of New York, 2900 Bedford Avenue, Brooklyn, NY 11210, USA

²Advanced Science Research Center at the Graduate Center, City University of New York, 85 St. Nicholas Terrace, New York, NY 10031 USA

10

Correspondence to: Vanessa.Alfonso23@bcmail.cuny.edu



15 Abstract

Late Cretaceous clays exposed at sites located on the north shore of Long Island, New York, USA were sampled to explore questions about how contemporary factors and processes interact with ancient geological materials. Chemically and biologically catalyzed weathering processes have produced multi-colored clays belonging to the kaolin group with inclusions of hematite, limonite, and pyrite nodules. We sampled exposed clays at three sites to address three questions: 1) Do these exposed clays support significant amounts of microbial biomass and activity, i.e., are they alive? 2) Do these clays support significant amounts of nitrogen (N) cycle activity? 3) Are these clays a potential source of N pollution in the contemporary landscape? Samples were analyzed for total carbon (C) and N content, microbial biomass C and N content, microbial respiration, organic matter (OM) content, potential net N mineralization and nitrification, soil nitrate (NO_3^-) and ammonium (NH_4^+) content, and denitrification potential. Results strongly support the idea that ancient geologic materials play a role in contemporary N and C cycling in the Critical Zone. Respiration was detectable in all samples and was strongly correlated to OM, indicating a living microbial community on the clays. There was evidence of an active N cycle. Higher levels of denitrification potential compared to both potential net nitrification and potential net N mineralization indicate that these clays act more as a sink rather than as a source of N pollution in the landscape.

1 Introduction

The Critical Zone is Earth's constantly evolving boundary layer where rock, soil, water, air, and living organisms interact (Schroeder, 2018). It is comprised of the solid phase matter in which water circulates and is stored, expanding from the top of the vegetation canopy down into the water bearing bedrock. Critical Zone processes are key drivers of chemical transfers between biota and geological materials (Brantley et al., 2006). A major question in Critical Zone science is how contemporary factors and processes interact with ancient geological materials. These interactions are influenced by the geochemical composition and pore space of these materials, which affect microbial activity and therefore rates of biogeochemical processes in the carbon (C) and nitrogen (N) cycles (Li et al., 2023). These interactions are particularly obvious and important in the lower boundary of the Critical Zone, and in places where ancient geologic materials become exposed to contemporary environments. Major questions center on the ability of ancient materials to support biogeochemical processes related to the cycling of C and N that underlie plant and microbial activity, which underlies environmental and ecosystem "services" of interest to society. The recent discovery of significant amounts of N in sedimentary deposits increased interest in the role of geological materials in contemporary N cycling (Morford et al., 2011). Up to 17% of the currently cycling N in some ecosystems may originate from rock materials deep in the Critical Zone (Houlton et al., 2018). Such observations motivate the analysis of surface-exposed ancient rocks in this study.



50 We measured microbial biomass and activity in clays exposed in outcrops with a focus on C and N cycle processes
to address three questions: 1) Do these exposed clays support significant amounts of microbial biomass and activity,
i.e, are they alive? To address this question we measured microbial biomass C, an index of the living microbial
biomass in soil, and microbial respiration, a direct measure of microbial activity (Paul, 2014). Total C and organic
matter (OM) content were measured as energy sources for microbial biomass and activity. 2) Do these clays support
55 significant amounts of N cycle activity? N cycle activity was assessed with measurements of microbial biomass N
content, potential net N mineralization, and total N content. Microbial biomass N provides an index of the net flux
of N through microbial pools. Mineralization results from microbial degradation of N compounds resulting in the
production of inorganic, plant-available forms of N. Total N content was measured to quantify the total amount of
N potentially available for active cycling. 3) Are these clays a potential source of N pollution in the contemporary
60 landscape? The potential for the clays' microbial activity to be a source or "sink" for N pollution was evaluated by
measuring potential net nitrification, denitrification potential, and pools of ammonium (NH_4^+) and nitrate (NO_3^-).
Both NH_4^+ and NO_3^- are highly soluble and the negative charge of NO_3^- makes it highly mobile, thus driving
hydrologic losses of N. In excessive amounts, these nutrients lead to ecological stresses such as eutrophication.
 NH_4^+ is converted to NO_3^- by nitrifying bacteria, and NO_3^- is converted to N_2 by denitrifying bacteria leading to
65 gaseous losses of N back into the atmosphere (Seitzinger et al., 2006).

2 Background

Silicates are the most abundant mineral group on Earth. Clay minerals are hydrous aluminosilicates, more
70 specifically hydrous phyllosilicates, and are some of the most stable products of chemical weathering at surface
conditions. Clay minerals make up approximately 40% of the minerals in sedimentary rocks, and about 16% of the
solid part of the Critical Zone. They are the constituents of soils, mudstones, claystones, and shales (Schroeder,
2018). Clay minerals produce a specialized microhabitat and their ability to store and release nutrients make them
ecologically important (Kleber et al., 2021). Clay minerals have high surface adhesion capabilities and sorption and
75 desorption of OM in soils varies with mineral assemblage. Sorption of organic carbon (OC) onto phyllosilicates and
hydrous iron (Fe) oxides affects accumulation and stabilization of OC in soils (Saidy et al., 2013). Ecosystem
function is greatly influenced by mineral abundances. The 1:1 layers of hydrated kaolinite clays and 2:1 layers of
mixed layer clays serve as nutrient exchange sites between biomass and subsurface weathering horizons. Therefore,
the layered structures of clays are key facilitators of seasonal cycling of nutrients including NH_4^+ among others
80 (Eby, 2016; Halama and Bebout, 2021). Chemical weathering of silicate minerals is a significant mechanism for the
availability, uptake, storage, and transport of key nutrients in ecosystems. Variations in mineral weathering and
nutrient availability occur due to microorganism and mineral speciation, while intensity of mineral weathering is
influenced by a mineral's potential to provide nutrients (P. C. Bennett et al., 2001). Nutrients are extracted from
rocks by weathering processes since rocks are the primary source of nutrients except C and N. The pathways of C
85 and N from the atmosphere to incorporation into the lithosphere progresses from fixation into OM to storage in low



temperature silicate phases such as clay minerals (Busigny and Bebout, 2013; Halama and Bebout, 2021). This is facilitated by the aqueous solutions and living microbes characteristic of the Critical Zone.

Late Cretaceous clays on the north shore of Long Island, New York, USA offer an opportunity to study the effects of contemporary factors and processes on ancient Critical Zone materials. Long Island is composed of Pleistocene sediments deposited on top of Late Cretaceous formations (Sirkin, 1991) and includes aquifers, confining units, and clay deposits such as the Raritan, Magothy, Gardiners, and Wantagh Clay Formations. Coastal exposures of the Raritan and Magothy formations present opportunities for biogeochemical analysis of these materials. At these locations clays are exposed in outcrops, offering the chance to investigate their contemporary biogeochemical activity at surface conditions (Fig. 1). Long Island's clay strata have been mainly accessed through core drilling for hydrological studies, and in most instances the clays are a secondary detail rather than the main subject of study. The same is true for palynology studies in which the clay is the assemblage containing the ancient pollens being studied. In contrast, this study focuses on biogeochemical activity and how the clay strata affect and interact with surrounding environments in the Critical Zone. The kaolinitic materials at these sites and their abundance in oxides contribute to long lasting micro-environments (Six et al., 2000).



Figure 1: Map of study sites on Long Island, New York. Map data: a) Esri, b) Google Earth.

All three study sites are located on the north shore of Long Island, NY. Two of the sites are located along the shoreline - Garvies Point Preserve (GP) on Hempstead Bay and Caumsett State Historic Park Preserve (CSP) along Long Island Sound; Hempstead Harbor Woods (HHW) is located inland from the western side of Hempstead Bay. Long Island contains numerous clay beds such as Gardiner's Clay, Raritan Confining Unit, Wantagh Clay, and Smithtown Clay, as well as clay lenses in the Magothy Formation (Mills and Wells, 1974). The study area was



shaped by the Wisconsin glaciation approximately 75,000 to 11,000 years ago. During this period, Cretaceous strata were sheared off, transported, and re-deposited. Glacially induced thrusting of the strata facilitated bulging of the clay (Mills and Wells, 1974), thus leading to eventual exposure. Evidence of this can be observed in the outcrop sampled for this study at GP, where the clay layers are currently oriented vertically rather than in a near horizontal depositional position. Although there is consensus that the Late Cretaceous deposits of the western north shore of Long Island were formed in a shallow delta or estuary (Fuller, 1914; Swarzenski, 1963) and that they are composed of sand, silt, gravel, and clay, further augmented by eolian action, it is not completely clear to which formation the exposed North Shore clays belong. It is generally accepted that the Late Cretaceous formations exposed on the North Shore tentatively belong to the Magothy formation but may include some younger formations (Isbister, 1966). It is presumed that Pleistocene deep permafrost formation must have preceded glacial thrusting (Mills and Wells, 1974), which provided the sedimentary cohesion needed to produce the tilted clay strata and layered shale observed today. The three sites of this study also differ in their position on the Manhasset Plateau. The HHW and GP localities are situated on the Upper Manhasset Plateau while CSP is situated on the Lower Manhasset Plateau. The Lower Manhasset Plateau is thought to have sustained a more prolonged grinding by the ice sheet (Fuller, 1914). The most abundant clay species identified from core drills in northwestern Long Island is kaolinite of light gray, brown-yellow, and tan color, along with sparse chlorite, vermiculite, and montmorillonite, with kaolinite ratio to other clays decreasing with depth (Liebling, 1973). Fe content, among other factors, has contributed to variations in coloring and produced distinctive clay strata, allowing for color based grouping of the samples. The color variations are the result of differences in constituents and geochemical processes that evolved the clays into their modern state. The Fe oxides in hematite are likely sources of the red and brownish coloring and the Fe oxides in goethite are likely sources of the yellow coloring (Davey et al., 1975). This is further supported by pXRF scan results (sections 4 and 5) which show red, yellow, and brown samples to have some of the highest Fe content. Mn also contributes to brown coloring (Jakobsson et al., 2000), and this is also further supported by pXRF scans that show brown samples to have the highest Mn content. Recent conditions have added sand and water to some clays to yield different textures, providing another observational classification criterion.

3 Methods

135

3.1 Study sites

Garvies Point Preserve (GP) is located in Glen Cove, NY, on the eastern shoreline of Hempstead Bay at 40°51'35" N 73°39'07" W. The exposed clays were accessed via trails leading to the beach and samples were collected along approximately 450 m of shoreline, with special focus on the main outcrop which features four types of clays exposed at this site. The most prominent outcrop at GP is approximately 4 m high and yielded samples from five differently colored clays (light gray, dark charcoal gray, white, yellow, and dark red/purplish). The adjacent outcrop is approximately 2 m high containing light and dark gray clay.



145 Hempstead Harbor Woods (HHW) is located in North Hempstead, NY, at 40°50'11" N 73°39'57" W, on the inland
western side of Hempstead Bay, approximately 300 m from the shoreline. Samples were collected from 0 – 1 m
from the ground level throughout the wooded area. Although this location does not have direct exposures to the bay,
some of the sampled clay materials have indicators of being part of the same formation as those exposed across the
bay at GP. Specifically, the red and light gray packed clays collected at HHW share the color and texture attributes
150 of those at GP.

At Caumsett State Historic Park Preserve (CSP) samples were collected from exposures along approximately 1000
m of shoreline. A prominent exposure at CSP located at 40°56'21" N 73°28'13" W has an elevation of
approximately 40 m. Samples were collected starting from the bottom of the cliff, just above the beach floor, and as
155 high as 6 m above the beach floor. Additional samples were collected from exposures at 40°56'08" N 73°28'14" W
approximately 4 m above the beach floor, and at 40°56'11" N 73°28'43" W approximately 6 m above the beach
floor.

3.2 Sampling

160 At each site samples were collected from locations that indicated the highest likelihood of yielding multiple clay
types. Large outcrops containing multiple variations of clay at GP and CSP were sampled more extensively. The
prominent outcrops at these locations feature variety in both color and texture. HHW featured scattered locations,
each featuring clay of a single texture and color. One sample from HHW (sample 3N-HHW) and one sample from
CSP (sample 1N-CSP) were collected from naturally exposed soil horizons (B horizon) underneath topsoil (O
165 horizon).

Samples were collected from the surface of the exposures. Locations where clay had at least a few inches of depth
were chosen. The uppermost layer (~1 cm) was scraped off to ensure only clay was collected and to remove any
field debris such as loose soil, rocks, sand, and loose plant material. Samples were collected from approximately 5-
10 cm of depth. The samples were collected using a trowel, placed in labeled Ziplock bags, and packed loosely with
170 some air remaining in the bag. Rocks, roots, and leaves were removed by hand right after collection. The samples
were then refrigerated until laboratory processing. Samples were classified into groups of color (brown, dark grey,
light gray, red, white, yellow) and texture (packed clay, sandy clay, watery clay) by visual observation. The packed
clay was homogeneous, contained some moisture, and had a putty like texture that easily formed into a ribbon
several inches long. The sandy clay was drier and had fine sand mixed in. The watery clay was collected from a
175 small basin of waterlogged clay that was homogeneous, had very fine particles, and a thick viscous texture.



3.3 Laboratory analysis

180

Samples were analyzed for moisture content by oven drying for 24 hours at 105°C. Moisture content was used to calculate values for all variables on a per g of dry soil basis.

OM content was determined by Loss on Ignition (LOI). Oven dried samples were “ignited” at 450°C in a muffle furnace and % OM was calculated from weight loss after 8 hours of heating.

185 For elemental analysis by pXRF, samples were oven dried for 24 hours at 80°C, ground with a mortar and pestle, sieved through a #230 (63µm) sieve, and scanned with a portable Olympus DC-4000 XRF scanner.

Total C, total N, and the C/N ratio were measured using flash combustion / oxidation. Oven dried and ground samples were pressed into 1g pellets. The pellets were analyzed in an Elementar varioMax Cube elemental analyzer.

190 For analysis of exchangeable NO_3^- and NH_4^+ , samples were blended with 2M KCl on an orbital shaker at 125 rpm for one hour, followed by filtration (Whatman #42 filter) into scintillation vials that were immediately refrigerated until analysis. The samples were pipetted into microplates and analyzed on a SpectraMax M2 Multi-Mode Microplate Reader from Molecular Devices using wavelengths of 450 nm for NO_3^- , and 650 nm for NH_4^+ (Doane and Horwath, 2003; Sims et al., 1995). Total inorganic N (TIN) was calculated as the sum of NH_4^+ and NO_3^- .

195 The chloroform fumigation and incubation method (CFIM) (Jenkinson and Powlson, 1976) was used to determine the C and N content of microbial biomass. Samples (10 g) were fumigated with chloroform for 24 hours, inoculated with 0.2 g of unfumigated clay and incubated for 10 days in 946 ml “mason” jars with lids fitted with septa. At the end of the incubation, gas samples were taken by syringe and analyzed for carbon dioxide (CO_2) with a Shimadzu GC-2014 gas chromatograph. After gas sampling, fumigated soils were extracted using KCl as described above
200 after 10 days and the NO_3^- and NH_4^+ produced over the 10 day incubation was taken as an estimate of microbial biomass N. A proportionality constant of 0.41 was used to calculate microbial biomass C from the CO_2 produced over the 10 day incubation.

Unfumigated samples were also incubated for 10 days and provided estimates of microbial respiration and potential net N mineralization and nitrification. These samples were incubated and sampled as described above and
205 production of CO_2 during the 10 day incubation was taken as an estimate of microbial respiration. Production of NO_3^- and NH_4^+ over the 10 day incubation was taken as an estimate of potential net N mineralization and production of NO_3^- was taken as an estimate of potential net nitrification.

A denitrification enzyme assay (DEA) was used to measure the rate of potential denitrification (Smith and Tiedje, 1979; Groffman et al., 1999). Samples were placed in 125 mL Erlenmeyer flasks and amended with NO_3^- , glucose
210 as a source of C / energy, and chloramphenicol to block production of new enzymes during incubation. The flasks were sealed with rubber stoppers, flushed repeatedly with N_2 gas to create anaerobic conditions, amended with acetylene (C_2H_2) gas, and placed on a shaker at 125 rpm. The headspace of the flasks was sampled (8 mL) by



syringe after 30 minutes and 90 minutes of incubation. Samples were analyzed for nitrous oxide (N₂O) with a Shimadzu GC-2014 gas chromatograph.

215

3.4 Statistical analysis

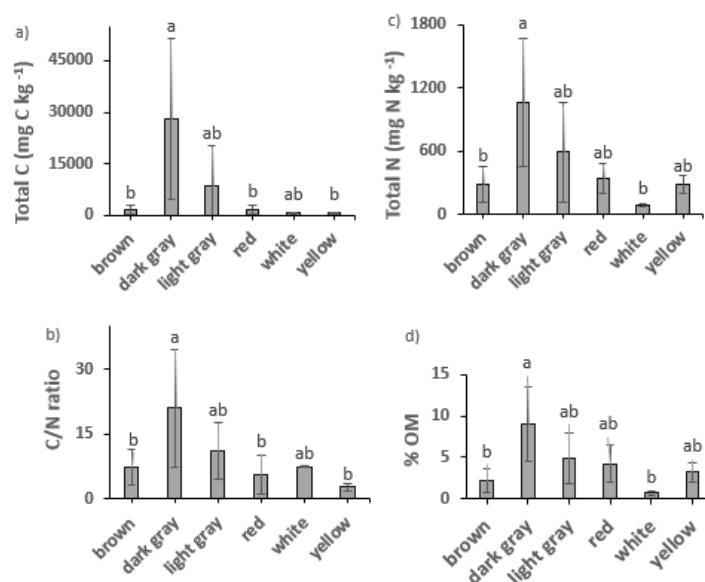
SPSS version 28 was used for all analyses. One-way analysis of variance (ANOVA) with post hoc multiple comparison tests were run on all response variables using location (GP, HHW, CSP), texture (packed, sandy, watery), and color (yellow, white, red, light gray, dark gray, brown) as grouping factors. A Sidak adjustment was applied to the post hoc multiple comparison tests because the number of samples was not equal across groups. Spearman's rho was used to evaluate linear correlations because the data were not normally distributed and had a heavy positive skew. ANOVA pretest results for homogeneity of variance were reinforced with Welch and Brown – Forsythe tests. Kruskal Wallis analysis was run to increase confidence in results for groupings by color, texture, and location. Mann-Whitney analysis with the Monte Carlo option was used to further reinforce ANOVA results grouped by location. Significance levels were evaluated based on $\alpha < 0.01$ indicating a strong statistically different significance, $\alpha < 0.05$ indicating a standard statistically different significance, and $\alpha < 0.1$ indicating a marginal statistically different significance. Since ANOVA results yielded the same significance parameters for the majority of variables as Kruskal Wallis and Mann-Whitney tests, ANOVA values are reported in the results section. Any variables that yielded significant differences only from ANOVA analysis are notated.

230

4 Results

All samples had detectable amounts of total C, N, and OM (Fig. 2). The dark gray samples had significantly higher OM, total C, total N, and C/N ratio than several of the other clay color types. The packed clay had the highest values of all these variables among the texture groups, and significant differences were found for OM between packed and sandy clays. ANOVA post hoc analysis identified further significant differences in the C/N ratio when comparing dark gray clay to the Fe bearing red, yellow, and brown clays. A number of packed, dark gray and light gray samples contained concentrations of N exceeding 1000 mg N kg⁻¹ which is considered ecologically significant for geologic N (Holloway and Dahlgren, 2002).

235



240

Figure 2: Total C, N, OM content, and C/N ratio of different colored clays. Values are mean ± SD. Values with different superscripts are significantly different ($p < 0.05$) except: in total C dark gray clay was marginally different ($p < 0.10$) from yellow clay; in total N dark gray clay was marginally different ($p < 0.10$) from brown and white clays; C/N ratio in dark gray clay was marginally different ($p < 0.10$) from brown clay.

245

pXRF scans yielded semi-quantitative results for selected elements of interest (Table 1). P was highest in brown clay and in watery clay with marginal differences between GP and HHW. Cl was highest in yellow, brown, and red clays, and in watery clays with significant differences among color groups and locations. Ti was highest in yellow, red, and brown clays, and in packed clays with significant differences among packed and sandy clay textures and marginal differences between GP and CSP locations. Mn was highest in brown clays and watery clays, with significant differences among color groups, textures, and locations. Fe was highest in brown, red, yellow clays, and in watery clays, with significant and marginal differences among color groups and locations. Rb was highest in dark gray, and in packed clays with significant differences among color groups and locations. Sr was similar across color groups with the highest concentrations in the light gray, dark gray, brown, and yellow samples. Zr was highest in brown and white samples and in sandy and watery clays, with significant and marginal differences among color groups, textures, and locations. Zn was highest in brown and dark gray, and in watery clays, with significant and marginal differences among color groups and locations. The Rb/Sr ratio was highest in dark gray clays, nearly the same across textures, with significant differences among color groups and locations (locations had additional marginal differences). There were significant correlations between P and Cl, P and Mn, P and Fe, Cl and Mn, Cl and Fe, Ti and Zr, Mn and Fe, Mn and Zn, Zn and Rb, Zn and Sr, Rb and Sr, Sr and Zr, and marginal correlations between P and Ti, and Ti and Fe.

250

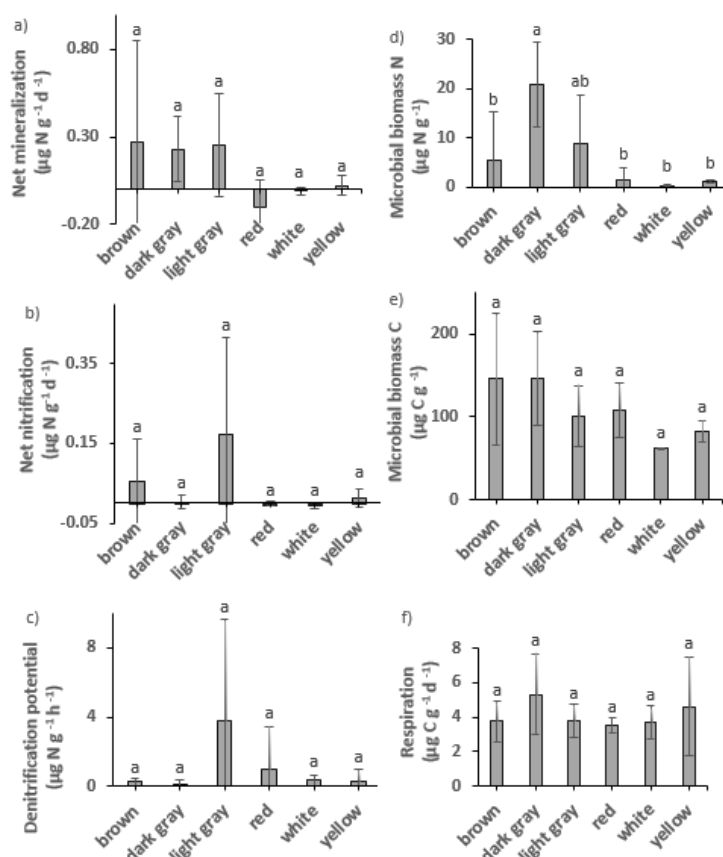
255

260



Garvies Point	P	Cl	Ti	Mn	Fe	Rb	Sr	Zr	Zn	Rb/Sr ratio
dark gray	10991.38	140312.87	4171.20	67.73	6736.80	139.20	73.93	288.47	65.47	1.89
light gray	3372.50	133413.83	3441.33	49.33	4820.00	111.33	70.17	284.33	45.17	1.56
red	30710.67	161559.78	4884.67	52.33	27106.89	98.67	67.67	294.67	48.56	1.46
white	9194.00	126827.67	4351.00	85.67	6296.33	137.00	75.67	335.33	48.33	1.81
yellow	25721.33	160147.78	4566.11	54.00	16648.44	110.33	72.22	340.44	34.00	1.52
Hempstead Harbor Woods										
brown	14576.00	152885.00	3806.00	204.67	14309.00	93.67	80.33	330.00	73.00	1.17
light gray	8068.67	123039.50	3832.17	40.17	6617.50	96.61	76.56	376.56	34.06	1.37
red	5371.50	139207.00	4649.67	23.33	7586.33	42.67	41.00	448.33	33.67	1.04
white	442.00	135305.00	3644.33	32.33	4786.33	79.67	51.00	804.67	23.00	1.56
Caumsett State Park										
brown	31116.83	161317.92	3584.17	352.92	25723.83	98.08	72.08	676.67	74.75	1.39
red	3942.00	142768.00	3741.00	81.00	18065.67	67.33	62.33	387.00	59.67	1.08

Table 1: Amounts of selected elements of interest detected by pXRF analysis; values are means in ppm.



265

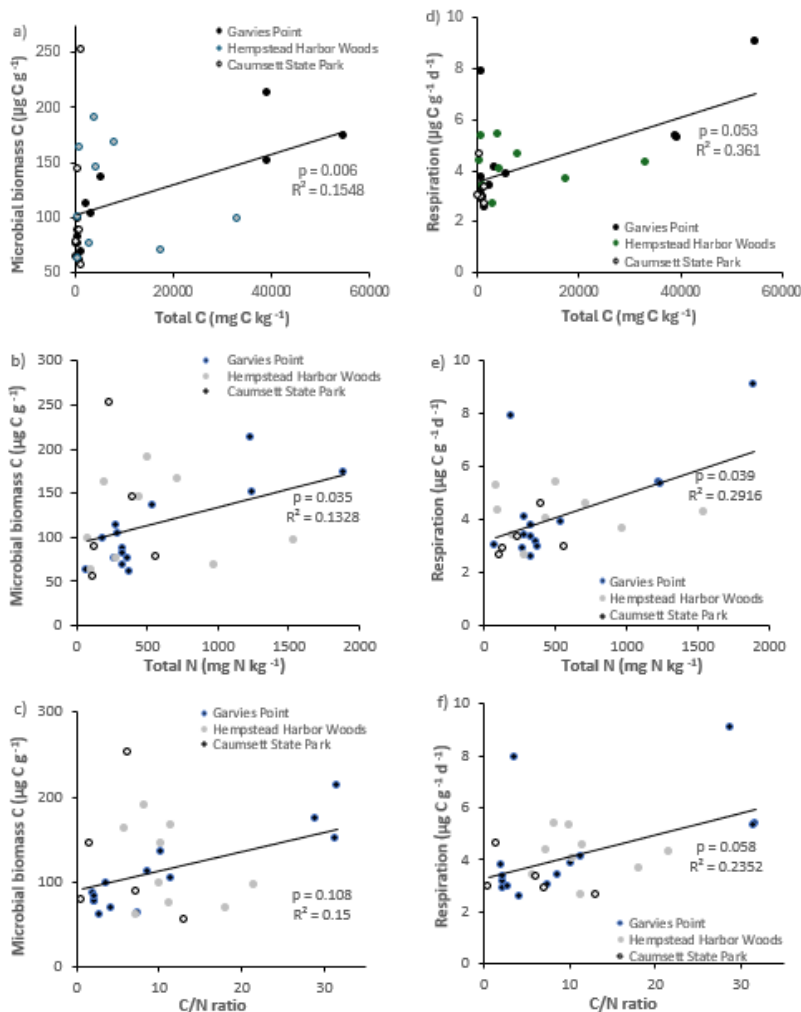
Figure 3: Microbial biomass and activity in clays classified by color: a) potential net N mineralization, b) potential net nitrification, c) denitrification potential, e) microbial biomass C, and f) respiration. Statistically different values occur in d) microbial biomass N, where values with different superscripts are significantly different at $p < 0.05$ except that dark gray clay was marginally different ($p < 0.10$) from brown and white clays. All values are mean \pm SD.



270

Most clay types exhibited detectable amounts of microbial biomass and activity (Fig. 3). Microbial biomass C was significantly higher in the watery clay than in the packed or sandy clay. A significant difference between watery and sandy clays was identified by ANOVA post hoc analysis. There were no significant differences in microbial biomass C with clay color. Soil respiration was detectable in all materials but there were no significant differences with clay color or texture. There were significant correlations between microbial biomass C and total N, total C (Fig. 4), OM, and respiration. Respiration was significantly correlated with total N (Fig. 4) and OM, and was also marginally correlated with total C and C/N ratio (Fig. 4).

275

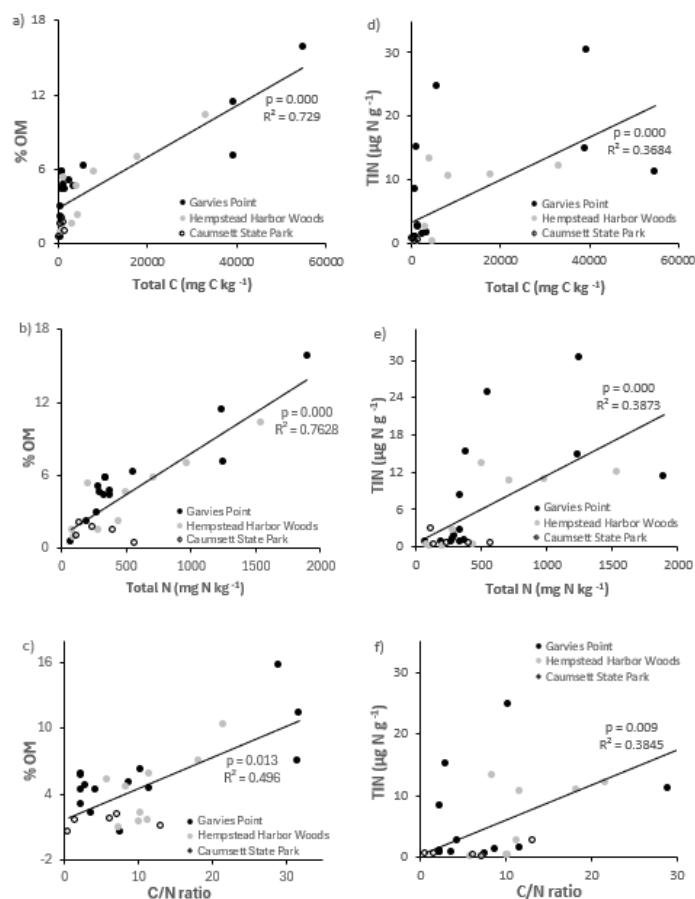


280 **Figure 4: Regression of microbial biomass C and respiration against total C, total N, and C/N ratio. Values are represented for each location; trendline is indicated among all locations. Significant differences occur where $p < 0.05$.**



285 There were significant differences in microbial biomass N among textures, and amounts were highest in dark gray and packed clays. We detected both potential net N mineralization and N immobilization (negative net N mineralization) in our samples (Fig. 3). Potential net N mineralization was highest in brown and in packed clays, with significant differences among samples from all locations. Net N mineralization was marginally different between the GP and HHW locations.

290 Microbial biomass N was significantly correlated with total C, total N, C/N ratio (Fig. 6), potential net nitrification, OM, and TIN. Total N was significantly correlated with microbial biomass C, and respiration (Fig. 4), OM, TIN (Fig. 5), microbial biomass N, potential net N mineralization (Fig. 6), and total C. Potential net N mineralization was significantly correlated with total C, total N, C/N ratio (Fig. 6), TIN, microbial biomass N, and potential net nitrification. Total N and the C/N ratio were marginally correlated.



295 **Figure 5: Regression of OM and TIN against total C, total N, and C/N ratio. Values are represented for each location; trendline is indicated among all locations. Significant differences occur where $p < 0.05$.**

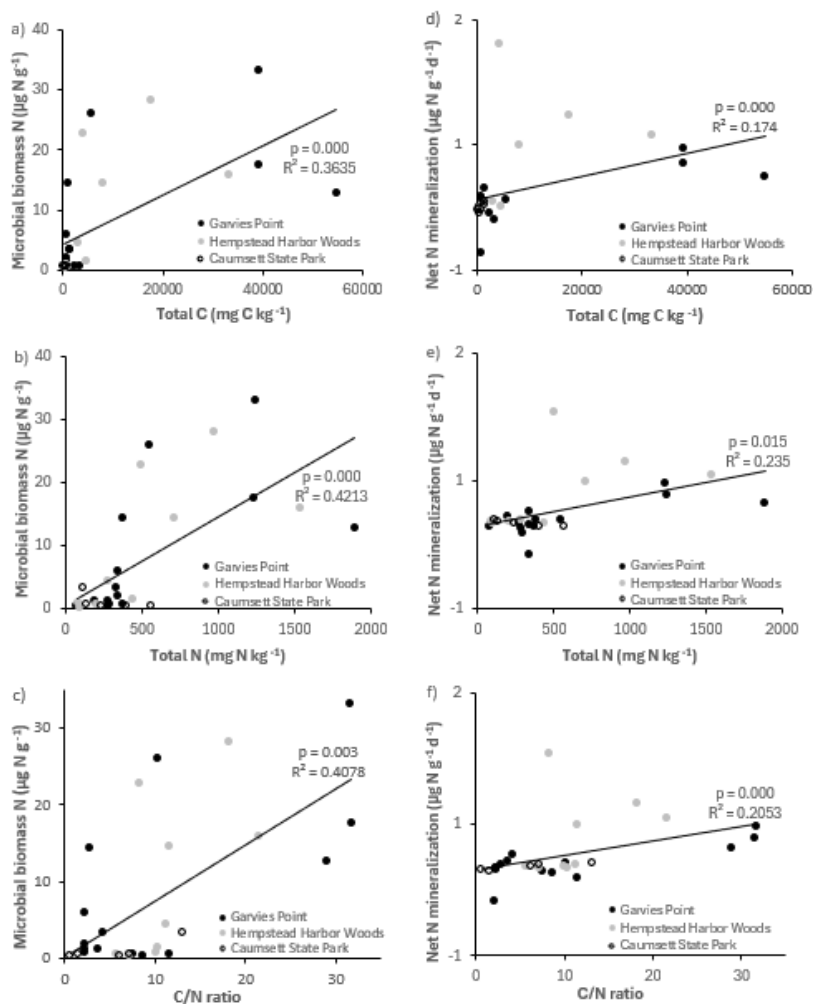
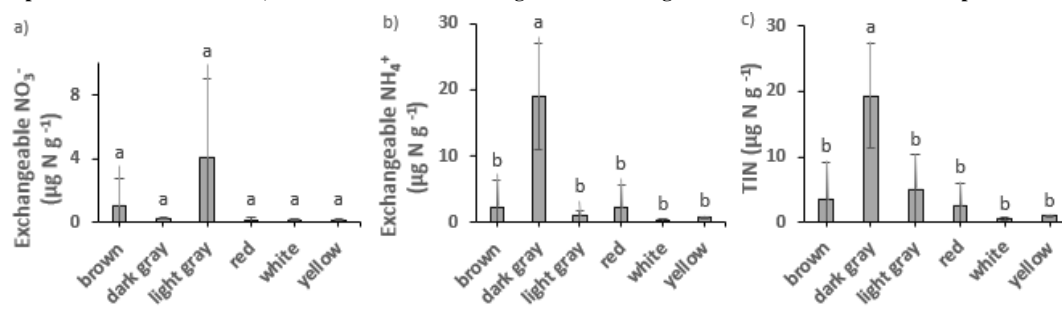


Figure 6: Regression of microbial biomass N and net N mineralization against total C, total N, and C/N ratio. Values are represented for each location; trendline is indicated among all locations. Significant differences occur where $p < 0.05$.



300 Figure 7: Exchangeable NO_3^- , NH_4^+ , and TIN in clays of different colors. Values are means \pm SD. Values with different superscripts are significantly different at $p < 0.05$.



The highest amounts of potential net nitrification were found in light gray (Fig. 3) and packed clays, with significant differences between the GP and HHW locations identified by ANOVA post hoc analysis. The highest amounts of
305 NO_3^- were found in light gray (Fig. 7) and packed clays, with significant differences between GP and HHW, and
between HHW and CSP identified by ANOVA post hoc analysis. The highest amounts of NH_4^+ were found in dark
gray (Fig. 7) and packed clays, with significant differences among color groups. The highest amounts of TIN were
found in dark gray and packed clays, with significant differences among color and texture groups. Kruskal Wallis
analysis identified a marginally significant difference for TIN by location. There were no significant differences in
310 denitrification potential.

Potential net nitrification was significantly correlated with total C, C/N ratio (Fig. 8), microbial biomass N, potential
net N mineralization, and marginally correlated with TIN. Denitrification potential was significantly correlated with
the C/N ratio (Fig. 8), suggesting joint control by C and N availability. There were significant correlations between
 NH_4^+ pools and the following variables: total C, total N, C/N ratio (Fig. 9), microbial biomass N, potential net N
315 mineralization, TIN, and OM. NO_3^- pools were significantly correlated with total N (Fig. 9), microbial biomass N,
and potential net N mineralization. There was a marginal correlation between NO_3^- and total C (Fig. 9).

5 Discussion

Our study sought to explore organic-mineral interactions by investigating the functional performance of clays
320 through measurements of biogeochemical processes occurring within their structures. This research aimed to
expand knowledge beyond the traditional approach of investigating C and N cycle dynamics based on single
predictor values such as phyllosilicate clay, abundance of a certain mineral species, and specific surface area and
adsorption values (Kleber et al., 2021) by making a suite of measurements of microbial biomass and activity
relevant to C and N cycles. This approach allowed us to determine that ancient clays are contributing to
325 contemporary Critical Zone biogeochemical processes at ecosystem and landscape scales.

5.1 N, C, and OM in geological materials

Over geological time scales, N and C cycle from the Earth's surface to depth through subduction zones and are
returned to the surface through arc magmatism. Geological cycling of N is greatly facilitated by storage of NH_4^+ in
silicate minerals. NH_4^+ in minerals is a major influence on fluxes between reservoirs (Halama and Bebout, 2021),
330 thus giving geological materials such as the clays we have analyzed a potential role in ecosystem function.

For contemporary ecosystem processes, it is generally assumed that geologic materials are not an important source
of N (Schlesinger, 2013), as the dominant global pool of N is in the atmosphere. The focus of much N cycle
research is on the energetically expensive movement of atmospheric N into biological pools (Galloway et al., 2004).
335 The largest pools of N in ecosystems are in particulate and dissolved OM pools in soils, sediments, and the ocean
(Groffman et al., 2021). Recently, recognition of the fact that much of this organic N becomes incorporated into



geological materials has fueled interest in the role of these materials in contemporary ecosystem processes. Recent analyses show that 10^{21} g of global fixed N were incorporated into sedimentary rocks by the burial of OM in marine and freshwater sediments (Morford et al., 2011). These analyses have stimulated studies of the movement of deeply buried organic N into actively cycling pools of N in soils and vegetation (Houlton et al., 2018) and interest in the exposure of ancient materials at the soil surface, such as the clays collected for this study.

At our study sites, burial of OM likely occurred in a Late Cretaceous shallow delta (Fuller, 1914). The N content of these samples is within the range of previous reports of sedimentary and metasedimentary rock N content of 200 – 1200 mg N kg⁻¹ (Holloway and Dahlgren, 2002; Morford et al., 2011). Organic-rich marine sediments commonly exceed 1000 mg N kg⁻¹ and some of our samples fit this criterion (Li, 1991; Morford et al., 2011). As these bedrock materials weather, N is released in plant available forms that stimulate ecosystem productivity and C storage (Dahlgren, 1994; Morford et al., 2011). Bedrock is also a source of N to aquifers, which is relevant for our samples which have a hydrogeologic origin from exposures of aquifer margins in a region with great concern about groundwater N pollution (Karamouz et al., 2020).

The surface exposure of the clays in our study allowed us to directly measure microbial biomass and activities that are central to biogeochemical cycling of C and N. These measurements shed light on the role that these secondary minerals, that were produced by the weathering of primary silicate minerals which originated at depth, may be playing in the contemporary N cycle on Long Island and in the Critical Zone elsewhere on Earth. These measurements also allowed for comparison of these geological materials with surface and subsurface soils in the region that have been assayed with the same methods (Groffman et al., 2009; Morse et al., 2014). Our analysis showed significant microbial biomass and activity in many samples, with much of the variation in activity driven by the total C and N content of the samples. The results strongly support the idea that ancient geologic materials play a role in contemporary N and C cycling in the Critical Zone.

Biogeochemical processes are influenced by microbial-mineral associations that influence the rates and magnitudes at which biogeochemical reactions occur. The structure of the mineral space influences the extent of biologically mediated reactions occurring within this habitat. Clays are expected to support less of these processes due to their tightly bound layered structure and fine particle size (Kleber et al., 2021). This is consistent with the lower amounts of activity detected in our samples compared to other soils, discussed in section 5.2. The tight structure of the clay offers a micro-environment that is more constant over time, as compared to the more dynamic conditions found within soil (Kleber et al., 2021). The longevity of a micro-environment is affected by both OM and mineralogy, with kaolinitic 1:1 clays and oxides producing longer lasting environments (Six et al., 2000). The smaller pore size of clay facilitates anaerobic conditions leading to higher denitrification rates in clay rich materials than in sandy ones (Li et al., 2023; Pihlatie et al., 2004). This relationship between particle size and microbial activity was evident in the analysis results obtained from our samples.



What then are the sources of the OC supporting microbial biomass and activity in the samples in this study, which varied with clay color and texture? Most C in coarse clay (0.2 – 2.0 μm) has been documented to be in the form of charcoal or black carbon (BC) (Laird et al., 2008). We have observed BC within the clay layers at the GP site, both distinctly layered with white clay and as small inclusions in some of the gray clay. This presence indicates that BC has become incorporated into silt and clay fraction minerals in the geological unit that is exposed at the GP site, through processes such as adsorption of dissolved biogenic compounds onto the clay particle surfaces (Laird et al., 2008).

380

Clay color is also affected by Fe, which likely contributed to the pigmentation of the red, yellow, and brown clays in our study. Our pXRF scans detected Fe content as high as 4.55 % in some samples. Possible sources of Fe include oxidative reactions and organic ligand bonding, both of which can be catalyzed by bacteria. The Fe content of Long Island's aquifers is driven by processes that include oxidative dissolution of minerals such as pyrite (FeS_2) (Brown and Schoonen, 2004). Pyrite inclusions occur in the clays at these study sites, and our pXRF scans detected the presence of S in addition to the Fe in our samples. Chelation of ions and organic acids is common in the Critical Zone. In the presence of water, Fe is one of the metal ions that can chelate with organic acids and become mobilized through the subsurface (Schroeder, 2018). Furthermore, Fe, Ti, and Mn, all of which were detected in our samples, play a key role in mineral and organic oxidation reactions. Fe(II), FeO_2 , and TiO_2 bearing clays produce the highest amounts of reactive O species, which in turn react with organic C to transform soil and sediment OM, and to produce CO_2 as the end-product of organic C oxidation (Kleber et al., 2021). Mn oxides are the strongest naturally occurring oxidants and play an important role in organic C transformation (Remucal and Ginder-Vogel, 2014).

The much higher occurrence of significant differences among the clays when grouped by color and texture, as opposed to when grouped by location, indicates that land use history and other local characteristics have less or no effect, and that the main differentiator for microbial activity is the clay material itself and variations therein, such as Fe oxides, trace elements, and variations in clay speciation. It also indicates that the clays from the different locations are likely part of the same larger formation (presumably Raritan or Magothy).

400 **5.2 Are these ancient clays contributing to contemporary biogeochemical processes?**

Our study was driven by three questions, the first of which was the most fundamental: do these materials support living microbial biomass? Our analysis detected a living microbial community on most of the clay samples. There were strong positive relationships between total C content, total N content, and microbial biomass and activity. The dark gray clays had the highest total N, total C, and microbial biomass N, and microbial biomass C was highest in both dark gray and brown clays. White clays had the lowest contents of these variables, indicating that inclusions of Fe and C (discussed in section 5.1) in the clays play a role in their capacity to sequester C and N and support microbial biomass and activity.



410 While our clay samples had significant amounts of microbial biomass and activity, they were less “alive” than
 surface soils that have been studied across the northeastern U.S. Both surface organic and subsurface mineral
 horizons of fully developed soils often have substantial C and N pools (Bohlen et al., 2001), with variations in
 distribution. We compared the data of our clay samples to two studies that used the same analysis methods
 (Groffman et al., 2009; Morse et al., 2014) (Table 2), to elucidate the differences in microbial biomass and activity
 415 between different soils and the clays. In a comparison with forest, agricultural, and grassland soils in the Baltimore,
 Maryland metropolitan area, respiration and microbial biomass C of the clays (respiration $4.1 \mu\text{g C g}^{-1} \text{d}^{-1}$; microbial
 biomass C $114 \mu\text{g C g}^{-1}$; ratio 28) was closest to the agricultural soil (respiration $6.7 \text{ mg C kg}^{-1} \text{d}^{-1}$; microbial
 biomass C 224 mg C kg^{-1} ; ratio 33) (Groffman et al., 2009) and lower than the forest or grassland soils.

420 We further compared our results to soils in various spodic hydropedologic settings in a northern hardwood forest at
 the Hubbard Brook Experimental Forest, New Hampshire (Morse et al., 2014). These settings included typical
 podzols (T), bimodal podzols (Bi), Bh podzols (Bh), and seeps, and three depths (Oi/Oe, Oa/A; B horizons) were
 sampled. Common features of spodosols are complexation with Al and Fe (often organic complexation) and
 enrichment with Fe and Mn (Van Ranst et al., 2018), thus sharing some elemental features with our clay samples
 425 since Al is a major constituent of clay and pXRF scans confirmed the presence of Mn and Fe in our samples.

		Total C	Respiration	MBC	MBN	NH ₄ ⁺	NO ₃ ⁻	TIN	ratio of MBC/Total C	ratio of MBC/Respiration
			mg C kg ⁻¹ d ⁻¹	MBC mg C kg ⁻¹		NH ₄ ⁺ mg N kg ⁻¹	NO ₃ ⁻ mg N kg ⁻¹	TIN mg N kg ⁻¹		
Groffman et al., 2009										
Forest mean			10.3	346		2.1	0.4	2.5		33.532
Agriculture mean			6.7	224		0.9	8.7	9.6		33.433
Grassland mean			8.2	306		0.5	1.2	1.7		37.317
Values source: Table 3										
Morse et al., 2014										
Hydropedologic setting	Horizon	Total C mg C kg ⁻¹	MBC ug C g ⁻¹	MBN ug N g ⁻¹	NH ₄ ⁺ ug N g ⁻¹	NO ₃ ⁻ ug N g ⁻¹	TIN ug N g ⁻¹	ratio of MBC/Total C		
T: typical podzols	Oi/Oe	506000	4780	774	152	16.8	168.8	0.009		
	Oa/A	329000	2320	320	30.4	18.3	48.7	0.007		
	mean of surface Oi/Oe, Oa/A	417500	3550	547	91.2	17.55	108.75	0.008		
	B > 10 cm	74000	481	32.4	2.4	3.33	5.73	0.007		
Bi: bimodal podzols	Oi/Oe	378000	6210	511	83.7	9.6	93.3	0.016		
	Oa/A	158000	1300	226	6.7	9.97	16.67	0.008		
	mean of surface Oi/Oe, Oa/A	269000	3755	368.5	45.2	9.785	54.985	0.012		
	B > 10 cm	56000	275	21.6	2.12	0.53	2.65	0.005		
Bh: Bh podzols	Oi/Oe	443000	6230	710	144	17.8	161.8	0.019		
	Oa/A	234000	3310	333	4.33	15.9	20.83	0.014		
	mean of surface Oi/Oe, Oa/A	338500	5770	521.5	74.465	16.85	91.315	0.016		
	B > 10 cm	60000	569	36	1.46	2.67	4.13	0.009		
Seep	Oa/A	232000	5060	238	9.18	1.02	10.2	0.022		
Values source: Table 1										
This study		Total C mg C kg ⁻¹	ug C g ⁻¹ d ⁻¹	MBC ug C g ⁻¹	MBN ug N g ⁻¹	NH ₄ ⁺ ug N g ⁻¹	NO ₃ ⁻ ug N g ⁻¹	TIN ug N g ⁻¹	ratio of MBC/Total C	ratio of MBC/Respiration
All locations, surface, mean		8220.18	4.1	113.53	7.64	4.63	1.47	6.11	0.014	27.690

HPS: hydropedologic setting, T: typical podzols, Bi: bimodal podzols, and Bh: Bh podzols; MBC: microbial biomass C, MBN: microbial biomass N.

430 **Table 2: comparison of response variables from this study to data from Groffman et al., 2009 and Morse et al., 2014. All three studies used the same sample analysis. Respiration and microbial biomass C of the clays in this study was closest to agricultural soils in the Baltimore, Maryland area (Groffman et al., 2009), and most comparable to the B horizon of the Bi setting at Hubbard Brook Experimental Forest, New Hampshire (Morse et al., 2014).**

Our samples, all of which were collected from the surface, were most comparable to the B horizons and to the Bi setting from Morse et al. (2014) (Table 2). B horizons in the Bi setting soils had the lowest total C and microbial biomass C and N contents of the Hubbard Brook soils but were still much higher than our clay values. The clay had



435 a higher microbial biomass C / total C ratio (0.014) than the surface (0.012) and B (0.005) horizons at Hubbard
Brook suggesting relatively high OM quality in the clays.

Morse et al., (2014), found that differences in total C and N content were more notable across soil horizons than
across hydrogeologic setting, where the B horizon, which accumulated Al and Fe, had less C and N and microbial
440 biomass and activity. The dominance of chemical (OM quality) versus location controls is consistent with the
stronger differences that we observed with color than with location. The composition of OM in clay fractions differs
from that in sand and silt fractions, and there is usually a decrease in C/N ratio as particle size decreases from coarse
silt to fine clay (Laird et al., 2008). In clay, the packed textures dominated by smaller particle size contain more OM
than larger particle sandy samples, but the C/N ratio increases with smaller particle size. In our samples, dark gray
445 clays had the highest total N, total C, and microbial biomass N; microbial biomass C was highest in both dark gray
and brown clays. White clays had the lowest contents of these variables, indicating that inclusions (such as Fe, BC,
and others) in the clays play a role in increasing their capacity to accommodate C and N rich contents.

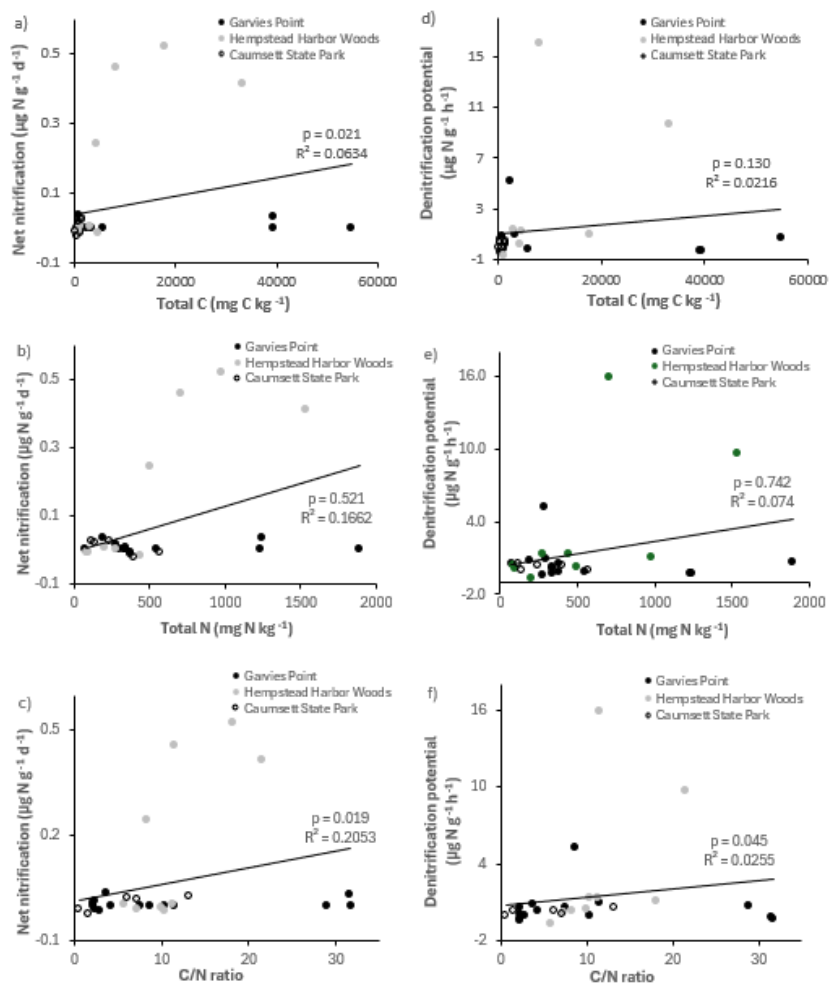
The second question our study addressed is whether the clays support an active N cycle. We measured several
450 indices of N cycling activity that showed that the exposed clays do indeed support an active N cycle and have
potential to supply N to support plant growth. Microbial biomass N is an index of the size of the actively cycling
labile N pool in soil. Mineralization, the production of simple, soluble, inorganic forms of N that are a dominant
source of N for plant growth, is strongly tied to the C cycle (Hart et al., 1994). When microbes degrade N
containing compounds during mineralization, their N is converted to proteins which release ammonia (NH_3) that
455 converts to NH_4^+ , and their C is converted to biomass or CO_2 (Groffman et al., 2021).

Microbial biomass N was highest in dark gray and packed clays, and correlated with potential mineralization and
nitrification, as well as with NH_4^+ , NO_3^- , TIN, and total N. Potential net N mineralization was highest and
comparable in brown and light gray and dark gray clays, and lowest in yellow clays. Microbial biomass N, potential
460 mineralization and nitrification, NH_4^+ , TIN, and total N were all strongly correlated with total C, and NO_3^- was
marginally correlated with total C, indicating C content as a driver in the coupling of these processes in the clays.
Microbial biomass N, potential mineralization, and nitrification were also correlated with OM. Respiration had a
stronger correlation with total N than with total C, but the strongest correlation was with microbial biomass C, and
there was no correlation between respiration and microbial biomass N. The C/N ratio was also highest in dark gray
465 and packed clays and lowest in Fe rich red and yellow, and in watery clays.

Our findings have general similarities to those of Morse et al. (2014), who found that clay rich B horizons have
lower rates of biogeochemical activity (lower net N mineralization and net nitrification potentials) as well as smaller
C and N pools than surface soils with less clay and Al. Clay minerals play a role in the C and N adsorption and
470 stabilization in soil. The storage potential of C is influenced by the size of the silicate mineral's surface area and the
amount of cations adhering to these minerals (Kahle et al., 2002). Adsorption rates and amounts of OM on mineral



surfaces are influenced by variations in aqueous solution dynamics, mineralogy, and OM chemistry, while OM affects mineral growth, transformation, and dissolution (Kleber et al., 2021).



475

Figure 8: Regression of net nitrification and denitrification potential against total C, total N, and C/N ratio. Values are represented for each location; trendline is indicated among all locations. Significant differences occur where $p < 0.05$.

480

The third question we asked is whether the clays are a source of N pollution. There is great concern about N pollution of groundwater and coastal waters in our region of study (Karamouz et al., 2020). There is particular concern about NO_3^- , the most highly mobile form of reactive N that is a drinking water pollutant and a prime cause of eutrophication in coastal waters (Conley et al., 2009). We therefore assessed the potential of these clays to contribute to high levels of NO_3^- in the environment by measuring both NO_3^- pools as well as processes that produce (nitrification) and consume (denitrification) NO_3^- .

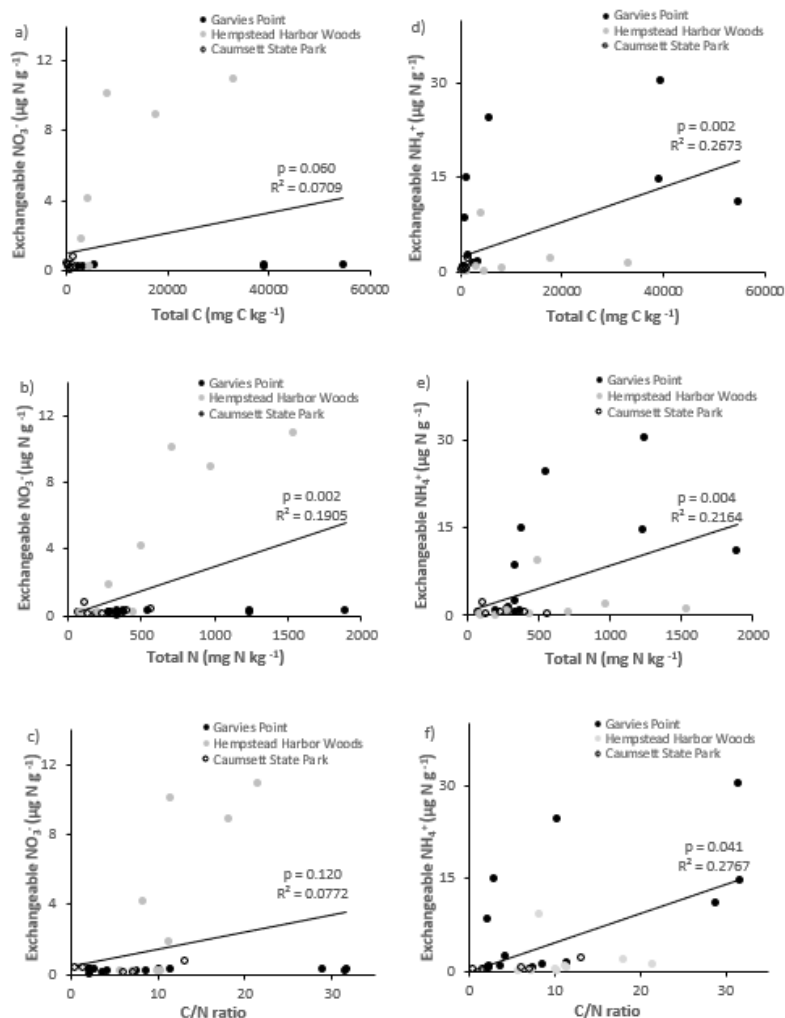


485

Nitrification is carried out by chemoautotrophic bacteria that oxidize NH_4^+ into NO_2^- which is further oxidized into NO_3^- . When this process is stimulated by the addition of N through application of fertilizers, atmospheric deposition, groundwater and runoff sources, it can lead to excessive production of NO_3^- (Groffman et al., 2021).

490

Denitrification is an anaerobic process that converts NO_3^- to gaseous forms NO , N_2O , N_2 (Robertson and Groffman, 2015), removing reactive N from the soil and facilitating the cycling of N between the biosphere and lithosphere to the atmosphere.



495

Figure 9: Regression of exchangeable NO_3^- and NH_4^+ against total C, total N, and C/N ratio. Values are represented for each location; trendline is indicated among all locations. Significant differences occur where $p < 0.05$.



5.3 N Pollution

500

N pollution occurs in the air, soil, and water. In the air it is the addition of volatile forms of N gasses, such as NO_y caused by industrial and commercial activity; in soil there is often an overload of nutrients from overuse of fertilizers and deposition from the atmosphere; in water a major cause is sewage system drainage and agricultural runoff, causing eutrophication which leads to dead zones in the oceans, in the most extreme scenario. The main

505

source for N pollution (in the form of NO₃⁻) to Long Island's aquifers is from septic systems, with additional inputs from agriculture, lawn care, and atmospheric deposition (Szymczycha et al., 2017). NO₃⁻ fluxes in Long Island's aquifers can negatively impact coastal ecosystems (Karamouz et al., 2020) and drinking water quality. The clay units included in Long Island's aquifer and aquitard strata can act as confining units, and as sinks or sources of N pollution.

510

The clays examined in this study could act as a minor source or a potentially significant sink for N pollution in an aquifer system. Clays with significant rates of potential net nitrification (especially the light gray clay) could be a source of NO₃⁻ if they were in contact with the aquifer. However, rates of denitrification potential were generally much higher than potential net nitrification, suggesting that these clay materials are more likely to act as NO₃⁻ sinks. The light gray clays have the potential to act as both NO₃⁻ sources and sinks depending on environmental conditions,

515

while the white and Fe-bearing (red, yellow) clays have the potential to act as NO₃⁻ sinks.

6 Conclusions

520

This investigation shed light on the amount and type of microbial activity that occurs in geological microhabitats in the Critical Zone at a coastal exposure of temperate northern latitude and allowed us to evaluate their potential local and regional impact.

Our analyses have taken a step towards better understanding the nature and extent of the biogeochemical activity that these types of microhabitats support. The approach of using laboratory measurements of microbial biomass and activity in ancient materials was successful in characterizing the biogeochemical potential of these materials, even at low levels, and could be applied in other Critical Zone studies.

525

The results from this study provide quantitative data showing microbial activity of silt and clay fraction materials of hydrogeologic origin, and confirm that these materials contain ecologically significant concentrations of geologic N exceeding 1000 mg N kg⁻¹ (Holloway and Dahlgren, 2002). Their surface exposure allowed us to explore the interaction between ancient geological stratigraphic components and modern day environmental conditions. This type of interaction is illustrative of the conceptual reach of Critical Zone science and the cohesive understanding of

530

multiple differing factors that it provides. The unity of various disciplines and their individual approaches to



investigation allow for greater understanding of the ensuing conditions that occur in the Critical Zone, where the resulting processes work together to support all living organisms.

Our results advance the emerging science of the geological N cycle and clearly show that ancient geological materials are contributing to contemporary biogeochemical processes in the Critical Zone of our study region.

535 Further, we have shown that these materials support a wide range of N cycle processes encompassing mineralization, immobilization, nitrification, and denitrification. There is a clear need for further research on how clay physical and chemical characteristics influence the flows of N to and from clays and biogeochemical processes in the Critical Zone, and to see how these materials and processes are contributing to the growth of vegetation and the dynamics of pollutants in the Critical Zone of this dynamic, densely populated, and environmentally sensitive
540 region.

Data availability

The supplement to this article is available at doi : [10.5281/zenodo.12702768](https://doi.org/10.5281/zenodo.12702768)

545

Author contributions

VMA conceptualized the study, performed field work and sample collection, laboratory analyses, data analysis, and wrote the manuscript; PMG designed the study, provided laboratory methodology, access, and supplies, interpreted results, co-wrote, and revised the manuscript; ZC provided laboratory equipment and access, interpreted results, and
550 revised and edited the manuscript; DES interpreted results, revised and edited the manuscript.

Competing interests

None of the authors have any competing interests.

555 Acknowledgements

The authors thank Clare Kohler and Kaitlin McLaughlin for help with laboratory analyses; and Veronica Natale and Dr. Herbert Mills for help obtaining samples.



560 References

- Bohlen, P. J., Groffman, P. M., Driscoll, C. T., Fahey, T. J., and Siccama, T. G.: PLANT–SOIL–MICROBIAL INTERACTIONS IN A NORTHERN HARDWOOD FOREST, *Ecology*, 82, 965–978, [https://doi.org/10.1890/0012-9658\(2001\)082\[0965:PSMIIA\]2.0.CO;2](https://doi.org/10.1890/0012-9658(2001)082[0965:PSMIIA]2.0.CO;2), 2001.
- 565 Brantley, S. L., White, T. S., White, A. F., Sparks, D. L., Richter, D., Pregitzer, K. S., Derry, L. A., Chorover, J., Chadwick, O. A., April, R., Anderson, S. P., and Amundson, R. C.: Frontiers in exploration of the critical zone. Report of a Workshop Sponsored by the National Science Foundation(NSF), Newark, DE, 30, 2006.
- Brown, C. J. and Schoonen, M. A. A.: The origin of high sulfate concentrations in a coastal plain aquifer, Long Island, New York, *Appl. Geochem.*, 19, 343–358, [https://doi.org/10.1016/S0883-2927\(03\)00154-9](https://doi.org/10.1016/S0883-2927(03)00154-9), 2004.
- 570 Busigny, V. and Bebout, G. E.: Nitrogen in the Silicate Earth: Speciation and Isotopic Behavior during Mineral-Fluid Interactions, *Elements*, 9, 353–358, <https://doi.org/10.2113/gselements.9.5.353>, 2013.
- Conley, D. J., Paerl, H. W., Howarth, R. W., Boesch, D. F., Seitzinger, S. P., Havens, K. E., Lancelot, C., and Likens, G. E.: Controlling Eutrophication: Nitrogen and Phosphorus, *Science*, 323, 1014–1015, <https://doi.org/10.1126/science.1167755>, 2009.
- 575 Dahlgren, R. A.: Soil acidification and nitrogen saturation from weathering of ammonium-bearing rock, *Nature*, 368, 838–841, <https://doi.org/10.1038/368838a0>, 1994.
- Davey, B. G., Russell, J. D., and Wilson, M. J.: Iron oxide and clay minerals and their relation to colours of red and yellow podzolic soils near Sydney, Australia, *Geoderma*, 14, 125–138, [https://doi.org/10.1016/0016-7061\(75\)90071-3](https://doi.org/10.1016/0016-7061(75)90071-3), 1975.
- 580 Doane, T. A. and Horwath, W. R.: Spectrophotometric Determination of Nitrate with a Single Reagent, *Anal. Lett.*, 36, 2713–2722, <https://doi.org/10.1081/AL-120024647>, 2003.
- Downey, A. E., Groffman, P. M., Mejía, G. A., Cook, E. M., Sritairat, S., Karty, R., Palmer, M. I., and McPhearson, T.: Soil carbon sequestration in urban afforestation sites in New York City, *Urban For. Urban Green.*, 65, 127342, <https://doi.org/10.1016/j.ufug.2021.127342>, 2021.
- 585 Eby, N.: Principles of environmental geochemistry, Waveland Press, Inc, Long Grove, Illinois, 514 pp., 2016.
- Fuller, M.: *The Geology of Long Island, New York*. Myron L. Fuller, *J. Geol.*, 24, 303–304, <https://doi.org/10.1086/622335>, 1914.
- Galloway, J. N., Dentener, F. J., Capone, D. G., Boyer, E. W., Howarth, R. W., Seitzinger, S. P., Asner, G. P., Cleveland, C. C., Green, P. A., Holland, E. A., Karl, D. M., Michaels, A. F., Porter, J. H., Townsend, A. R., and Vorosmarty, C. J.: Nitrogen Cycles: Past, Present, and Future, *Biogeochemistry*, 70, 153–226, <https://doi.org/10.1007/s10533-004-0370-0>, 2004.
- Groffman, P. M., Holland, E. A., Myrold, D. D., Robertson, G. P., and Zou, X.: “Denitrification.” In Standard soil methods for long-term ecological research, Oxford University Press, New York, 272–288 pp., 1999.
- 595 Groffman, P. M., Williams, C. O., Pouyat, R. V., Band, L. E., and Yesilonis, I. D.: Nitrate Leaching and Nitrous Oxide Flux in Urban Forests and Grasslands, *J. Environ. Qual.*, 38, 1848–1860, <https://doi.org/10.2134/jeq2008.0521>, 2009.
- Groffman, P. M., Rosi, E. J., and Fulweiler, R. W.: The nitrogen cycle. In K. C. Weathers, D. L. Strayer, & G. E. Likens (Eds.), in: *Fundamentals of Ecosystem Science*, Academic Press, 161–188, 2021.



- 600 Halama, R. and Bebout, G.: Earth's Nitrogen and Carbon Cycles, *Space Sci. Rev.*, 217, 45, <https://doi.org/10.1007/s11214-021-00826-7>, 2021.
- Hart, S. C., Nason, G. E., Myrold, D. D., and Perry, D. A.: Dynamics of Gross Nitrogen Transformations in an Old-Growth Forest: The Carbon Connection, *Ecology*, 75, 880–891, <https://doi.org/10.2307/1939413>, 1994.
- Holloway, J. M. and Dahlgren, R. A.: Nitrogen in rock: Occurrences and biogeochemical implications: BIOGEOCHEMICAL IMPLICATIONS OF N IN ROCK, *Glob. Biogeochem. Cycles*, 16, 65-1-65–17, <https://doi.org/10.1029/2002GB001862>, 2002.
- 605 Houlton, B. Z., Morford, S. L., and Dahlgren, R. A.: Convergent evidence for widespread rock nitrogen sources in Earth's surface environment, *Science*, 360, 58–62, <https://doi.org/10.1126/science.aan4399>, 2018.
- Jakobsson, M., Løvlie, R., Al-Hanbali, H., Arnold, E., Backman, J., and Mörth, M.: Manganese and color cycles in Arctic Ocean sediments constrain Pleistocene chronology, *Geology*, 28, 23, [https://doi.org/10.1130/0091-7613\(2000\)28<23:MACCIA>2.0.CO;2](https://doi.org/10.1130/0091-7613(2000)28<23:MACCIA>2.0.CO;2), 2000.
- 610 Jenkinson, D. S. and Powelson, D. S.: The effects of biocidal treatments on metabolism in soil—V, *Soil Biol. Biochem.*, 8, 209–213, [https://doi.org/10.1016/0038-0717\(76\)90005-5](https://doi.org/10.1016/0038-0717(76)90005-5), 1976.
- Kahle, M., Kleber, M., and Jahn, R.: Review of XRD-based quantitative analyses of clay minerals in soils: the suitability of mineral intensity factors, *Geoderma*, 109, 191–205, [https://doi.org/10.1016/S0016-7061\(02\)00175-1](https://doi.org/10.1016/S0016-7061(02)00175-1), 2002.
- 615 Karamouz, M., Mahmoodzadeh, D., and Oude Essink, G. H. P.: A risk-based groundwater modeling framework in coastal aquifers: a case study on Long Island, New York, USA, *Hydrogeol. J.*, 28, 2519–2541, <https://doi.org/10.1007/s10040-020-02197-9>, 2020.
- 620 Kleber, M., Bourg, I. C., Coward, E. K., Hansel, C. M., Myneni, S. C. B., and Nunan, N.: Dynamic interactions at the mineral–organic matter interface, *Nat. Rev. Earth Environ.*, 2, 402–421, <https://doi.org/10.1038/s43017-021-00162-y>, 2021.
- Laird, D. A., Chappell, M. A., Martens, D. A., Wershaw, R. L., and Thompson, M.: Distinguishing black carbon from biogenic humic substances in soil clay fractions, *Geoderma*, 143, 115–122, <https://doi.org/10.1016/j.geoderma.2007.10.025>, 2008.
- 625 Li, L., Shields, J., Snow, D. D., Kaiser, M., and Malakar, A.: Labile carbon and soil texture control nitrogen transformation in deep vadose zone, *Sci. Total Environ.*, 878, 163075, <https://doi.org/10.1016/j.scitotenv.2023.163075>, 2023.
- Li, Y. H.: Distribution patterns of the elements in the ocean: A synthesis, *Geochim. Cosmochim. Acta*, 55, 3223–3240, [https://doi.org/10.1016/0016-7037\(91\)90485-N](https://doi.org/10.1016/0016-7037(91)90485-N), 1991.
- 630 Liebling, R. S.: Clay Minerals of the Weathered Bedrock Underlying Coastal New York, *Geol. Soc. Am. Bull.*, 84, 1813, [https://doi.org/10.1130/0016-7606\(1973\)84<1813:CMOTWB>2.0.CO;2](https://doi.org/10.1130/0016-7606(1973)84<1813:CMOTWB>2.0.CO;2), 1973.
- Mills, H. C. and Wells, P. D.: Ice-Shove Deformation and Glacial Stratigraphy of Port Washington, Long Island, New York, *Geol. Soc. Am. Bull.*, 85, 357, [https://doi.org/10.1130/0016-7606\(1974\)85<357:IDAGSO>2.0.CO;2](https://doi.org/10.1130/0016-7606(1974)85<357:IDAGSO>2.0.CO;2), 1974.
- 635 Morford, S. L., Houlton, B. Z., and Dahlgren, R. A.: Increased forest ecosystem carbon and nitrogen storage from nitrogen rich bedrock, *Nature*, 477, 78–81, <https://doi.org/10.1038/nature10415>, 2011.
- Morse, J. L., Werner, S. F., Gillin, C. P., Goodale, C. L., Bailey, S. W., McGuire, K. J., and Groffman, P. M.: Searching for biogeochemical hot spots in three dimensions: Soil C and N cycling in hydrogeologic settings in a



- 640 northern hardwood forest: Biogeochemical hotspots in soil profiles, *J. Geophys. Res. Biogeosciences*, 119, 1596–1607, <https://doi.org/10.1002/2013JG002589>, 2014.
- P. C. Bennett, Rogers, J. R., Chol, W. J., and Hiebert, F. K.: Silicates, Silicate Weathering, and Microbial Ecology, *Geomicrobiol. J.*, 18, 3–19, <https://doi.org/10.1080/01490450151079734>, 2001.
- Paul, E. A.: Soil microbiology, ecology, and biochemistry, Fourth edition., Academic Press, Amsterdam, 2014.
- 645 Pihlatie, M., Syväsalo, E., Simojoki, A., Esala, M., and Regina, K.: Contribution of nitrification and denitrification to N₂O production in peat, clay and loamy sand soils under different soil moisture conditions, *Nutr. Cycl. Agroecosystems*, 70, 135–141, <https://doi.org/10.1023/B:FRES.0000048475.81211.3c>, 2004.
- Remucal, C. K. and Ginder-Vogel, M.: A critical review of the reactivity of manganese oxides with organic contaminants, *Environ. Sci. Process. Impacts*, 16, 1247, <https://doi.org/10.1039/c3em00703k>, 2014.
- 650 Robertson, G. P. and Groffman, P. M.: Nitrogen transformations., in: *Soil Microbiology, Ecology, and Biogeochemistry.*, Academic Press, Burlington, MA, 421–446, 2015.
- Saidy, A. R., Smernik, R. J., Baldock, J. A., Kaiser, K., and Sanderman, J.: The sorption of organic carbon onto differing clay minerals in the presence and absence of hydrous iron oxide, *Geoderma*, 209–210, 15–21, <https://doi.org/10.1016/j.geoderma.2013.05.026>, 2013.
- Schlesinger, W. H.: An estimate of the global sink for nitrous oxide in soils, *Glob. Change Biol.*, 19, 2929–2931, <https://doi.org/10.1111/gcb.12239>, 2013.
- 655 Schroeder, P. A.: *Clays in the Critical Zone*, Cambridge university press, Cambridge New York, 2018.
- Seitzinger, S., Harrison, J. A., Böhlke, J. K., Bouwman, A. F., Lowrance, R., Peterson, B., Tobias, C., and Drecht, G. V.: DENITRIFICATION ACROSS LANDSCAPES AND WATERSCAPES: A SYNTHESIS, *Ecol. Appl.*, 16, 2064–2090, [https://doi.org/10.1890/1051-0761\(2006\)016\[2064:DALAWA\]2.0.CO;2](https://doi.org/10.1890/1051-0761(2006)016[2064:DALAWA]2.0.CO;2), 2006.
- 660 Sims, G. K., Ellsworth, T. R., and Mulvaney, R. L.: Microscale determination of inorganic nitrogen in water and soil extracts, *Commun. Soil Sci. Plant Anal.*, 26, 303–316, <https://doi.org/10.1080/00103629509369298>, 1995.
- Sirkin, L.: Stratigraphy of the Long Island Platform, *J. Coast. Res.*, 217–227, 1991.
- Six, J., Elliott, E. T., and Paustian, K.: Soil Structure and Soil Organic Matter II. A Normalized Stability Index and the Effect of Mineralogy, *Soil Sci. Soc. Am. J.*, 64, 1042–1049, <https://doi.org/10.2136/sssaj2000.6431042x>, 2000.
- 665 Smith, M. S. and Tiedje, J. M.: Phases of denitrification following oxygen depletion in soil, *Soil Biol. Biochem.*, 11, 261–267, [https://doi.org/10.1016/0038-0717\(79\)90071-3](https://doi.org/10.1016/0038-0717(79)90071-3), 1979.
- Swarzenski, W. V.: *Hydrogeology of Northwestern Nassau and Northeastern Queens counties, Long Island, New York*, USGS Geological Survey Water Supply Paper 1657, 88 pp., 1963.
- 670 Szymczycha, B., Kroeger, K. D., Crusius, J., and Bratton, J. F.: Depth of the vadose zone controls aquifer biogeochemical conditions and extent of anthropogenic nitrogen removal, *Water Res.*, 123, 794–801, <https://doi.org/10.1016/j.watres.2017.06.048>, 2017.
- Van Ranst, E., Wilson, M. A., and Righi, D.: Spodic Materials, in: *Interpretation of Micromorphological Features of Soils and Regoliths*, Elsevier, 633–662, <https://doi.org/10.1016/B978-0-444-63522-8.00022-X>, 2018.